ORIGINAL RESEARCH

Phytosynthesis of Silver Nanoparticles Using *Perilla frutescens* Leaf Extract: Characterization and Evaluation of Antibacterial, Antioxidant, and Anticancer Activities

NV Reddy[1]
Huizhen Li[1]
Tianyu Hou[1]
MS Bethu[2]
Zhiqing Ren[1]
Zhijun Zhang[1]

[1]School of Chemical Engineering and Technology, North University of China, Taiyuan, Shanxi Province, People's Republic of China; [2]Pharmacology and Toxicology Division, Indian Institute of Chemical Engineering and Technology, Hyderabad, Telangana State, India

Purpose: The present study investigates the phytosynthesis of silver nanoparticles (AgNPs) using *Perilla frutescens* leaf extract, which acts as a reducing agent for the conversion of silver ions (Ag+) into AgNPs. *P. frutescens* leaf synthesized AgNPs (PF@AgNPs) were evaluated for biomedical properties including antibacterial, antioxidant and anticancer activities.

Materials and Methods: PF@AgNPs were synthesized using *P. frutescens* leaf extract and silver nitrate solution. The morphology and physical properties of PF@AgNPs were studied by spectroscopic techniques including, UV-Vis, FTIR, TEM, XRD, DLS, and TGA. Antibacterial activity of PF@AgNPs was evaluated by disk diffusion assay. Antioxidant activity of PF@AgNPs was checked by 2.2-diphenyl-1-picrylhydrazyl (DPPH), and 2.2′-azino-bis (3-ethylbenzothiazoline-6-sulfonic acid) (ABTS) free radical scavenging assays. Anticancer activity of PF@AgNPs was checked by 3-(4,5-dimethylthiazol-2-yl)-2,5-diphenyl tetrazolium bromide assay. Cytotoxic effects of PF@AgNPs on most susceptible cancer cell lines were observed by phase contrast microscopy.

Results: PF@AgNPs showed surface plasmon resonance peak at 461 nm. XRD pattern showed that the PF@AgNPs were face-centered cubic crystals with a mean size of 25.71 nm. TEM analysis revealed the different shapes (spherical, rhombic, triangle, and rod) of PF@AgNPs. Zeta potential value (−25.83 mV) indicated that PF@AgNPs were long-term stable and not agglomerated. A low polydispersity index value (0.389) indicated the monodispersity of PF@AgNPs. TGA revealed the high thermal stability of PF@AgNPs. PF@AgNPs exhibited maximum inhibition against *Escherichia coli*, followed by *Bacillus subtilis* and *Staphylococcus aureus*. PF@AgNPs showed maximum inhibition of 68.02 and 62.93% against DPPH and ABTS-free radicals, respectively. PF@AgNPs showed significant anticancer activity against human colon cancer (COLO205) and prostate adenocarcinoma (LNCaP). PF@AgNPs exhibited apoptotic effects on LNCaP cells including cell shrinkage, membrane blebbing, chromatin condensation, fragmentation of nuclei, and formation of apoptotic bodies.

Conclusion: The present study reports the successful synthesis of PF@AgNPs using *P. frutescens* leaf extract. The synthesized PF@AgNPs are FCC crystals, monodispersed, long-term stable, and non-agglomerated. The observed antibacterial, antioxidant, and anticancer activities demonstrate the potential biomedical applications of PF@AgNPs.

Keywords: *Perilla frutescens*, silver nanoparticles, antibacterial activity, antioxidant activity, anticancer activity, LNCaP

Correspondence: Zhijun Zhang
School of Chemical Engineering and Technology, North University of China, Taiyuan, Shanxi Province 030051, People's Republic of China
Email sxzzj@163.com

Introduction

Owing to their unequivocal properties and promising features, nanomaterials will play essential roles in the future. Nanomaterials are used in drug delivery to increase the bioavailability, solubility, and half-life of drugs, and they have been widely employed for targeted and controlled release of drugs in cancer chemotherapy. Noble metals such as gold, platinum, silver, titanium, and palladium have been used extensively to synthesize nanomaterials.[1–3] Metallic nanoparticles, particularly silver nanoparticles (AgNPs), have gained importance because of their unique properties, including electronic, thermal, optical, magnetic, and catalytic attributes.[3–5] AgNPs have been widely used as bio-labeling materials, polarizing filters, biosensors, signal enhancers, optical receptors, and biocatalysts, and as antibacterial, antioxidant, anticancer, antiviral, antinociceptive, larvicidal, and insecticidal agents.[3–7] AgNPs have been widely employed in the preparation of medical kits, diagnostic kits, wound dressings, antiseptic creams, hand wash liquids, and bandages in the medical field because of the innate antimicrobial nature of silver.[8–11] The antimicrobial properties of AgNPs render them suitable for infusion into tissue/cartilage/bone grafting materials such as collagen, polycaprolactone, and hydroxyapatite.[12,13] The deodorant properties of AgNPs have been utilized in fabrics, sports shoes, and other sporting equipment.[14] AgNPs have been widely used in the coatings of walls, windows, timber furniture, glass, and countertops of hospitals to reduce the growth of bacteria and fungi.[15,16] The antioxidant and antimicrobial properties of AgNPs have been particularly useful in the preparation of food packing materials to increase the shelf life of foods and food ingredients.[17,18]

The physicochemical properties of AgNPs can be determined by their size, shape, surface area to volume ratio, and crystalline nature.[1,2,5] Various chemical and physical methods have been successfully employed for size- and shape-controlled synthesis of AgNPs, including laser ablation, thermal decomposition, lithographic, aerosol, UV-radiation, γ-irradiation, ultrasonication, microwave-assisted, photochemical, sonochemical, electrochemical, polyvinyl pyrrolidine, polyol, polyaniline, tollens process, and other chemical reduction methods.[4,5,19] However, chemical and physical methods for synthesis of nanoparticles involve hazardous chemicals and toxic radiations and require separate capping agents. Furthermore, toxic chemicals on the surface of AgNPs limit their biomedical applications.[20] Environmentally friendly methods for biological synthesis of AgNPs, including enzymatic, microbial, and plant-mediated synthesis, have become a new research avenue in the nanotechnology field worldwide. Although enzymatic methods are eco-friendly, they involve different steps, including isolation, extraction, and purification of enzymes, and are time-consuming, arduous, and expensive. Microbial methods involve laborious culturing conditions, and the mishandling of microbes can lead to contamination and risk to human health. Synthesis of non-toxic, clean, biocompatible, and biofunctionalized AgNPs using plant extracts deserves merit as a simple, rapid, cost-effective, eco-friendly, and safe method beings.[6,21,22]

Plants contain secondary metabolites, such as phenolic compounds, flavonoids, triterpenoids, alkaloids, quinines, coumarins, glycosides, steroids, and anthocyanins, that confer resistance to plants against pests, insects, drought stress, and other stress conditions. These compounds are very important for humans as they possess a wide variety of bioactivities, including anticancer, antioxidant, antidiabetic, anti-obesity, antibacterial, and antiviral properties.[23,24] Over the last two decades, scientists have successfully employed plant extracts and their secondary metabolites for the production of different types of metallic nanomaterials. In this simple, rapid, and cost-effective process, plant metabolites act as bioreduction agents that reduce the metal salts and metal oxides to their respective metallic nanoparticles. The plant metabolites also stabilize the nanoparticles by capping them.[6,19]

Perilla frutescens is a herbaceous perennial plant belonging to the family Lamiaceae. It is an important medicinal plant that is widely distributed in China, India, Korea, Japan, and Southeast Asia.[25] There are wild and cultivated varieties in the northern, southwestern, and other regions in China. The leaves of *P. frutescens* were used as a food ingredient in China. Perilla leaves have a wide variety of natural active substances including phenylpropanoids (elemicin, isoelemicin, myristicin, and methyl isoeugenol), alkaloids (1H-indole-3-carboxylic acid and indole-3-carboxaldehyde), phenolic compounds (rosmarinic acid, protocatechuic acid, caffeic acid, vanillic acid, and ferulic acid),[26] (Takano et al, 2004), flavonoids (luteolin, apigenin, scutellarein, catechin, negletein, vicenin-2, and catechin),[27–29] anthocyanins (shisonin, Cis-shisonin, and malonyl shisonin), coumarins (esculetin and 6.7-dihydroxycoumarin), carotenoids, neolignans, sesquiterpenoids, fatty acids, policosanols, tocopherols, sitosterols, glucosides, peptides, benzoxepin derivatives and other constituents.[26,30,31] The leaves of *P. frutescens* showed multiple biological functions due to the presence of

abundant natural active substances. The biological functions including antidiabetic activity (α-glucosidase and aldose-reductase inhibitory activity of luteolin, apigenin, and diosmetin),[28,32] anti-hyperuricemia (xanthine oxidase inhibitory activity of luteolin, negletein and scutellarin),[27] antispasmodic effect of flavonoid vicenin,[29] insecticidal activity of sesquiterpenoids,[30] antiallergic activity (hyaluronidase inhibition by rosmarinic acid, caffeic acid, and luteolin), anti-inflammatory activity of phenylpropanoids,[33] anti-depressant activity of luteolin and apigenin, hepatoprotective activity of caffeic acid and rosmarinic acid, antioxidant activity of flavonoids and polyphenols, anticancer and antimicrobial activities of triterpenoids, flavonoids, and polyphenols.[31,34–36] In the present investigation, we report the phytosynthesis of AgNPs using *P. frutescens* aqueous leaf extract, which acts as both a reducing and stabilizing agent for AgNPs. Characterization of AgNPs was achieved using a range of spectroscopic methods. The synthesized AgNPs were evaluated for antibacterial activities against gram-negative (*Escherichia coli*) and gram-positive (*Bacillus subtilis* and *Staphylococcus aureus*) bacteria using a disk diffusion assay. The antioxidant activity of the AgNPs was checked by 2,2-diphenyl-1-picrylhydrazyl (DPPH), and 2,2′-azino-bis (3-ethylbenzothiazoline-6-sulfonic acid) (ABTS) radical scavenging assays. The anticancer activity of the PF@AgNPs was evaluated against human colon cancer (COLO205) and human prostate adenocarcinoma (LNCaP) cell lines using an MTT (3-(4,5-dimethylthiazol-2-yl)-2,5-diphenyl tetrazolium bromide) assay.

Materials and Methods
Preparation of *P. frutescens* Leaf Extract and Phytosynthesis of PF@AgNPs

The leaves of *P. frutescens* were collected from croplands near the North University of China, Taiyuan, Shanxi Province, China. Initially, *P. frutescens* leaves were washed thoroughly with tap water and then rinsed with distilled water for 10 to 15 min. Finally, the leaves were cleaned with double distilled water (DDW) and then dried completely under shade. The dried leaves were crushed into a fine powder. Leaf powder (10 g) was added to 100 mL of DDW in a 250 mL flask and then boiled at 50°C for 30 min.[37,38] Subsequently, the solution was allowed to cool to room temperature and filtered by employing simple filtration process through Whatman No.1 filter paper. The filtrate, named as *P. frutescens* leaf

aqueous extract, was used for the phytosynthesis of PF@AgNPs. This extract (10 mL) was added to 2 mM AgNO$_3$ (90 mL), and the mixture was boiled at 50°C for 30 min and then incubated for 2 h in the dark.[37,38] The light yellow color of the solution became dark brown after incubation.

Spectral Analysis of PF@AgNPs

To confirm phytosynthesis, the dark brown colloidal solution was analyzed using ultraviolet–visible (UV–Vis) spectroscopy (Perkin-Elmer Ltd) between 200 and 800 nm.[39] After confirmation of phytosynthesis, the solution of PF@AgNPs was centrifuged for 20 min at 15,000 × g. The supernatant was removed and the pellet was redispersed in distilled water and centrifuged again for 20 min at 15,000 × g. This procedure was repeated for three times.[40] Finally, the pellet was collected and dried into a fine powder that was used for further analysis. Fourier transform infrared (FTIR) analysis of PF@AgNPs was carried out at 4000–500 cm^{-1} using KBr pellets (Perkin-Elmer Ltd).[41] The x-ray diffraction (XRD) pattern of PF@AgNPs was recorded in the 2θ range of 10° to 90° using Bruker D8 Advance powder XRD (Bruker AXS GmbH, Karlsruhe, Germany).[42] Thermogravimetric analysis (TGA) and derivative thermogravimetric analysis (DTA) were performed using a TGA-1 analyzer (Mettler Toledo, Switzerland).[43] The shapes and sizes of PF@AgNPs and the selected area electron diffraction (SAED) pattern of PF@AgNPs were determined using transmission electron microscopy (TEM).[44] The polydispersity index (PI) and zeta potential values were recorded using dynamic light scattering (DLS; Brookhaven Instruments).[45]

Antibacterial Activity of PF@AgNPs

For this study, we selected both gram-negative (*E. coli*) and gram-positive (*B. subtilis* and *S. aureus*) pathogens. Bacterial cultures were activated 24 h prior to the assay. The antibacterial activity of PF@AgNPs was evaluated using a Kirby–Bauer disk diffusion assay.[46] First, 10 mL of Luria-Bertani (LB) agar was added to Petri dishes under sterile laminar airflow (LAF). Then, 150 μL of active bacterial suspension was added to each LB agar plate. Thereafter, four sterile paper disks saturated with dimethyl sulfoxide (DMSO; control), 10 μL of PF@AgNPs, 10 μL of pristine leaf extract (PTLE), and 10 μL of streptomycin (standard antibiotic drug) were transferred onto LB plates and then incubated

at 37°C for 24 h. Inhibition zones were determined by measuring the bacterial clearance around each disk in mm.

Antioxidant Activity of PF@AgNPs

Antioxidant activity of PF@AgNPs was evaluated using DPPH and ABTS scavenging assays.[47,48] Ascorbic acid was used as the standard antioxidant. In DPPH assay, PF@AgNPs (20, 40, 60, 80, and 100 µg) were dissolved in 1 mL methanol in separate test tubes. Then, 2 mL DPPH stock solution (1 mM/L) was added, and the tubes were incubated in the dark for 45 min. Then, the absorbance values were recorded at 517 nm. In ABTS assay, ABTS radical working solution was prepared prior to the assay. ABTS radical working solution (0.9 mL) was added to 0.1 mL of the different concentrations (20, 40, 60, 80, and 100 µg/mL) of PF@AgNPs, shaken well for 45 sec, and incubated in the dark for 15 min, followed by measurement of the absorbance at 734 nm. DPPH/ ABTS scavenging activity was calculated using the equation: % scavenging = [(control absorbance − test compound absorbance)/control absorbance] × 100.

Anticancer Activity of PF@AgNPs

The anticancer activity of PF@AgNPs was evaluated by MTT assay using human colon cancer (COLO205) and human prostate adenocarcinoma (LNCaP) cell lines by the method of Mossman (1983).[49] The cells (5×10^3) were seeded in 96 well plates, with each well containing 100 µL of medium. After overnight incubation in a 5% CO_2 chamber at 37°C, exactly 100 µL of different concentrations of PF@AgNPs (10, 20, 40, 60, 80, and 100 µg/mL) were added. After 24 h, the cell viability was checked by the addition of 10 µL MTT per well and incubation for a further 3 h. The plates were centrifuged for 10 min at 1000 × g. Thereafter, the medium was discarded, and the formazan blue crystals formed were dissolved in dimethyl sulfoxide (100 µL). Then, the absorbance values were recorded at 570 nm, and the percentage of cell viability was determined. To study morphological changes, further phase-contrast images were taken of the most susceptible cell lines to PF@AgNPs at concentrations of IC_{25}, IC_{50}, and IC_{75} after 24 h of exposure.

Statistical Analysis

All the experiments were repeated for three times. Mean values were represented with standard deviation. Significance analysis between each group of data was carried out under the condition of $P<0.05$. Statistical analyses involved the use of SPSS version 22.0. We have employed Origin 8.5 for the interpretation of UV-Vis, FTIR, TGA, and XRD peaks. We have employed Prism 7.0 for drawing graphs.

Results and Discussion
Phytosynthesis of PF@AgNPs

In the present study, we investigate the phytosynthesis of AgNPs using *P. frutescens* leaf extract. This acts as a reducing agent to convert silver ions (Ag^+) into nanosilver (Ag^0), named as *P. frutescens* leaf-synthesized silver nanoparticles (PF@AgNPs). Phytosynthesis was initially observed by a color change of the reaction solution (containing silver ions and leaf extract) from a light-yellow color to dark brown color (Figure 1) after 2 h of incubation in the dark. This color change indicates the phytosynthesis of PF@AgNPs. Phytosynthesis was further confirmed by UV–Vis analysis. The resultant UV–Vis spectrum (Figure 2) showed a hyperbolic peak between 400 and 480 nm. This peak is a characteristic absorption peak of AgNPs due to surface plasmon vibrations excited by the silver metal lattice.[1,2,50] Phytochemicals such as flavonoids, triterpenoids, glycosides, and polyphenolic components might carry out the bioreduction of Ag^+ to Ag^0. The schematic diagram (Figure 3) depicts a possible mechanism of phytosynthesis of AgNPs that can be accomplished in three steps. The first activation step involves the reduction of silver ions (Ag^+) into metallic silver atoms (Ag^0). In the second step, nucleation and growth phases occur during which small

Figure 1 Color change of the reaction solution from light yellow to dark brown after 2 h indicates the formation of PF@AgNPs.
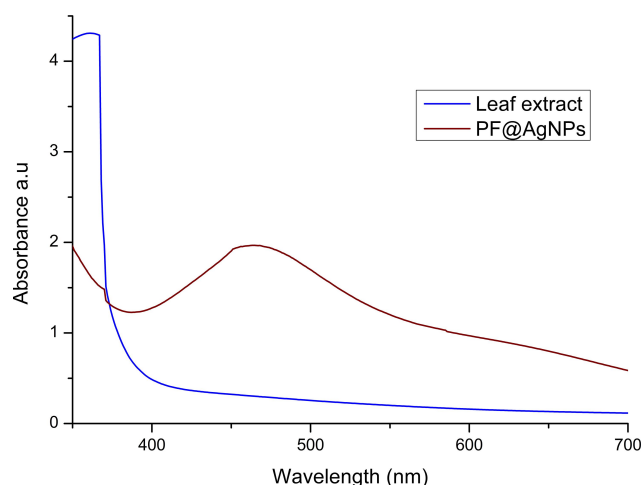
Figure 2 UV-Vis analysis of *P. frutescens* leaf extract and PF@AgNPs. UV-Vis spectrum of PF@AgNPs showed surface plasmon resonance peak at 461 nm.

adjacent metallic silver atoms coalesce into AgNPs of a definitive size and shape. The final step involves the stabilization process in which phytochemicals cap AgNPs, thus preventing their agglomeration.

Phytosynthesis of AgNPs has become popular owing to its economical, eco-friendly, and simple procedure. Phytosynthesized AgNPs have many advantages over chemically synthesized AgNPs (CS-AgNPs). Phytosynthesized

AgNPs do not require surface coating chemicals for stabilization. In CS-AgNPs, these surface coating chemicals lead to the formation of toxic and non-biocompatible AgNPs that cannot be used for various biomedical purposes (drug delivery, tissue grafting, bone regeneration, wound dressings, dental implants, diagnostic equipment, and other medical devices) as they contain toxic/hazardous chemicals on their surface. In contrast, phytosynthesis produces clean, non-toxic, and biocompatible AgNPs that can be used for various biomedical purposes.[19,22]

FTIR Analysis of Phytosynthesized PF@AgNPs

FTIR analysis was carried out to determine the major phytochemicals involved in the phytosynthesis and capping of PF@AgNPs. The FTIR spectrum (Figure 4A) of *P. frutescens* leaf extract showed peaks at 627, 821, 1048, 1381, 1608, 2386, 2926, and 3372 cm^{-1}. The FTIR spectrum (Figure 4B) revealed major peaks at 615, 1124, 1374, 1601, 2913, and 3385 cm^{-1}. The peaks at 627 and 615 cm^{-1} were due to the C-H group, which indicated the presence of aliphatic and aromatic compounds. The peaks at 1048 and 1124 cm^{-1} represented C-O (carboxylic acid) stretching vibrations of aromatic compounds. The peaks at 1381 and
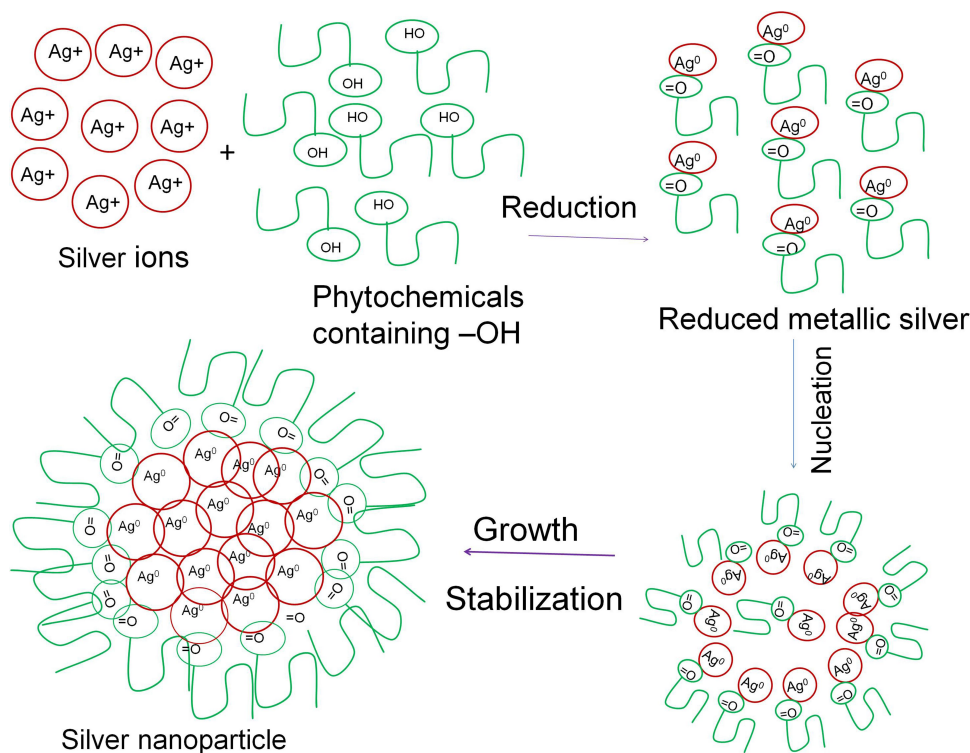

Figure 3 Schematic diagram represents the possible mechanism of plant-mediated synthesis (phytosynthesis) of AgNPs.
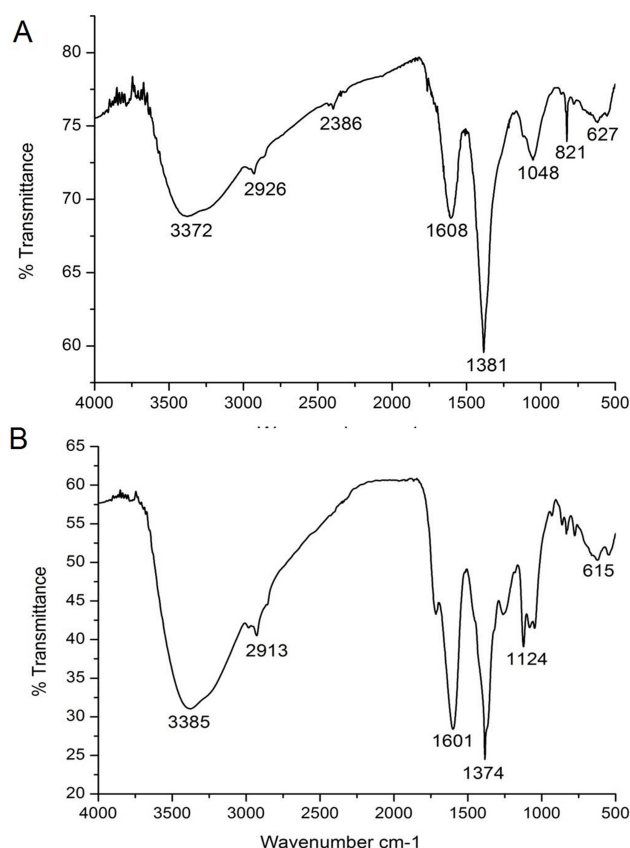
Figure 4 FTIR analysis of (**A**) *P. frutescens* leaf extract and (**B**) PF@AgNPs.

1374 cm^{-1} indicated C-N stretching vibrations of aromatic amines.[51] The peaks at 1608 and 1601 cm^{-1} signified the secondary amide (-N-H) group of peptide bonds. The shift in the peak from 627 to 615 cm^{-1} revealed the participation of aromatic/aliphatic compounds in the synthesis of PF@AgNPs. The shift in the peak from 1381 to 1374 cm^{-1} and shift in the peak from 1608 to 1601 cm^{-1} revealed the involvement of proteins, which cap around the AgNPs and act as stabilizing agents. Capped AgNPs are non-agglomerated and very stable for long durations. The stability of PF@AgNPs was further explained by DLS studies. The peaks at 2926 and 2913 cm^{-1} were due to the methylene (-C-H) group of aromatic/aliphatic chains.[52] The peaks at 3372 and 3385 cm^{-1} corresponded to the O-H (hydroxyl) group of flavonoids, triterpenoids, and phenolic compounds. This is a critical shift that demonstrates the involvement of polyphenolic compounds in the reduction of Ag$^+$ ions into AgNPs.[53] The disappearance of some peaks and shifting in the bands clearly demonstrate the involvement of polyphenols and proteins in the synthesis and stabilization of PF@AgNPs. Polyphenolic compounds such as rosmarinic acid, caffeic acid, protocatechuic acid,

chlorogenic acid, vanillic acid, ferulic acid, gallic acid, apigenin, and luteolin have been reported in the leaves of *P. frutescens*, and it is plausible that these compounds may be involved in the bioreduction process.[31] Phenolic acids possess a phenolic nucleus and a carboxyl group, and thus form a resonance stable phenoxy radical nucleus. Oxidation of phenolic acids leads to stable phenoxy radical formation.[54] Hence, oxidation of phenolic acids by AgNO$_3$ produces stable phenoxy radicals and reduced metallic silver atoms. The reduced metallic silver atoms join together and form a stable silver nanoparticle. A plausible mechanism of phytosynthesis and capping of AgNPs is depicted in the schematic diagram (Figure 3). Our FTIR results were consistent with previous reports, which demonstrated that polyphenolic compounds are involved in the bioreduction process and that proteins provide stability by capping them.[31,51–54]

XRD Pattern of Phytosynthesized PF@AgNPs

The crystal nature of metallic nanoparticles is a key factor affecting their proper biological functions. The XRD pattern of PF@AgNPs (Figure 5) showed major diffraction peaks at 38.11, 44.29, 64.39, and 77.32° that were indexed to (111), (200), (220), and (311) diffraction planes, respectively. The diffraction peaks and their respective planes revealed that the phytosynthesized PF@AgNPs were crystalline with a face-centered cubic (FCC) lattice (JCPDS File No. 4–0783). Crystallite size (nm) was determined using the Debye–Scherrer equation: crystallite size d=Kλ/β$_{0.5}$cosθ, where K is the Scherrer constant '0.95′, λ indicates source light wavelength (1.54 A°/0.54 nm), β$_{0.5}$ indicates the FWHM (full width half maximum length), and θ is the Bragg angle (radians). Using the Gaussian nonlinear curve fit (NLFfit), the FWHM of the nanocrystal was determined as 0.34215°. According to the Debye–Scherrer equation, the crystallite size (d) was 25.71 nm. Our XRD results were consistent with those of previous studies. AgNPs synthesized using *Tithonia diversifolia*,[52] *Artemisia turcomanica*,[53] and *Ziziphus Jujuba*,[55] are all nanocrystals with FCC structure.

TEM and DLS Analysis of Phytosynthesized PF@AgNPs

TEM micrographs (Figure 6A–E) revealed that the phytosynthesized PF@AgNPs in this study were 20–50 nm in size with various shapes, including spherical, rhombic,
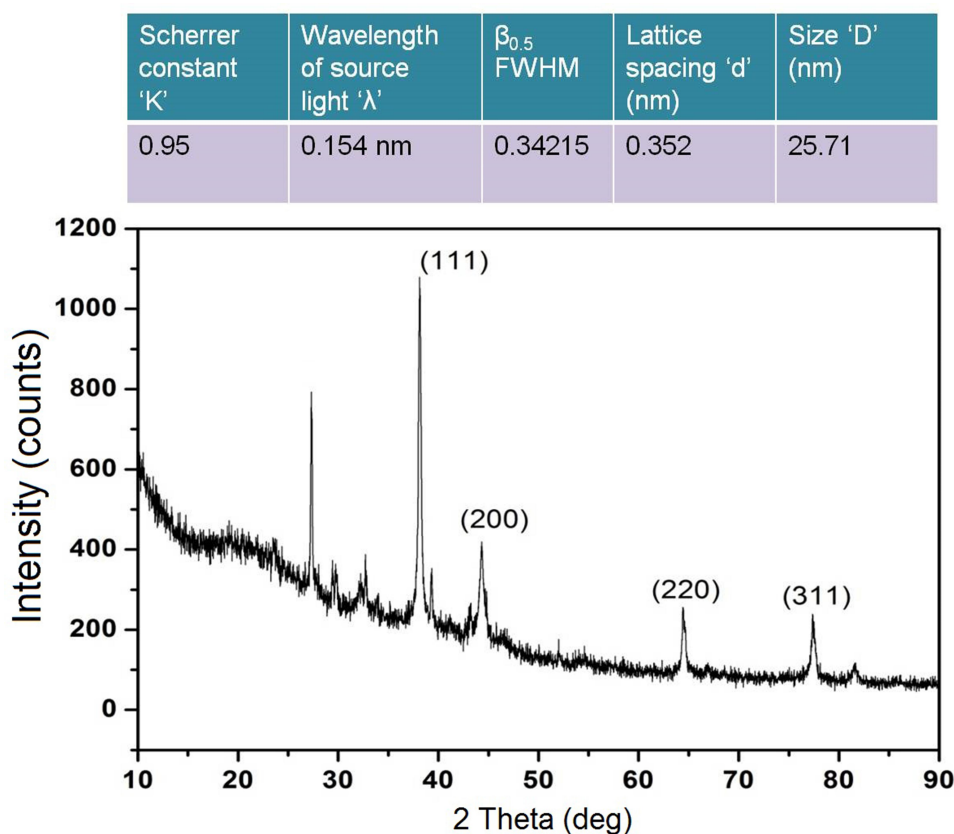
Scherrer constant 'K'	Wavelength of source light 'λ'	$\beta_{0.5}$ FWHM	Lattice spacing 'd' (nm)	Size 'D' (nm)
0.95	0.154 nm	0.34215	0.352	25.71

Figure 5 XRD pattern of PF@AgNPs.

triangle, and rod. However, most AgNPs were spherical. TEM micrographs also showed that PF@AgNPs were monodispersed with no aggregation. The SAED pattern (Figure 6F) of the nanocrystals showed clear Debye–Scherrer rings of FCC crystal. Our TEM results were consistent with those of previous studies. The sizes of AgNPs synthesized using *Artemisia turcomanica*,[53] *Ziziphus Jujuba*,[55] *Artemisia absinthium*,[56] *Berberis vulgaris*[57] are 20–60 nm, 20–30 nm, 5–20 nm, and 30–70 nm, respectively, and all are spherical.

DLS studies showed that the PI value of PF@AgNPs was 0.389, which indicated that PF@AgNPs are monodispersed. The stability of PF@AgNPs was further demonstrated by zeta potential (ZP) measurement (Figure 7). The ZP value of PF@AgNPs was −25.83 mV. This high negative ZP value revealed the repulsion between the AgNPs. The repulsion indicated that PF@AgNPs are long-term stable with no aggregation. TEM micrograph clearly showed the non-aggregation of PF@AgNPs and is due to capping of PF@AgNPs by proteins or phytochemicals of *P. frutescens* leaf extract. Our DLS results were consistent with those of previous reports. The PI and ZP values of

AgNPs synthesized using *Pterodon emarginatus*,[58] *Juglans regia*,[59] *Punica granatum*,[60] were, respectively, 0.372, 0.4, and 0.54 for PI, and −23.9, −33.8, and −34.3 mV for ZP. The DLS results support the monodispersity and long-term stability of phytosynthesized PF@AgNPs.

TG and DTG Analysis of Phytosynthesized PF@AgNPs

TG and DTG plots (Figure 8) were studied to determine the thermal stability of phytosynthesized PF@AgNPs. TG and DTG plots revealed that phytosynthesized PF@AgNPs were highly stable between 25 and 900°C with very low weight loss. The TG plot of PF@AgNPs revealed steady weight loss in the temperature range of 100–900°C. The DTG plot of PF@AgNPs showed that three major weight losses of 0.14, 0.24, and 0.18% were observed at 111.25, 180.75, and 328.75°C, respectively. The observed weight loss might be due to the desorption of weak conjugated phytochemicals with nanosilver. The TG and DTG results revealed that phytochemicals capped on the nanoparticles impart stability against temperature
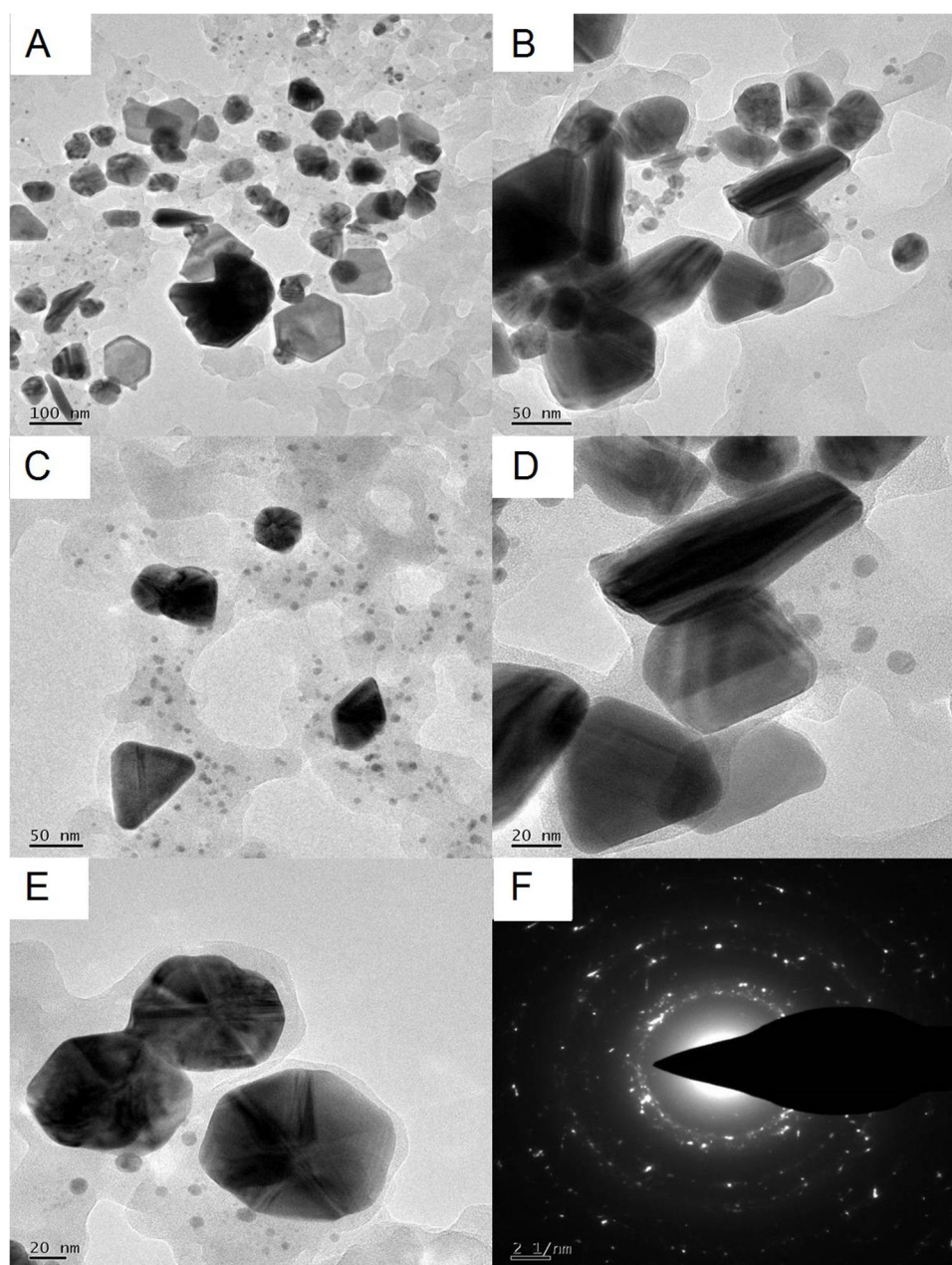
Figure 6 TEM analysis PF@AgNPs (**A**) TEM micrograph at 100 nm shows monodispersed AgNPs with different shapes including spherical, rod, triangle, and rhombic; (**B**) rod-shaped, rhombic shaped, and spiral-shaped AgNPs observed at 50 nm scale; (**C**) triangle, rhombic and spherical shaped AgNPs at 50 nm; (**D**) rod-shaped and triangle-shaped AgNPs at 20 nm; (**E**) spherical shaped AgNPs at 20 nm; (**F**) SAED pattern of AgNPs.

variations. These phytochemicals act as conjugated molecules on the surface of AgNPs.

Antibacterial Activity of PF@AgNPs

The antibacterial activity of PF@AgNPs was evaluated by a disk diffusion assay against *E. coli, B. subtilis*, and *S. aureus*. PF@AgNPs exhibited effective antibacterial activity against all the tested species and produced inhibition zones after 24 h of incubation. Figure 9 represents that PF@AgNPs produced inhibition zones of 14.4, 10.6, and 10.3 mm against *E. coli, B. subtilis*, and *S. aureus*, respectively. Antibacterial activity of the pristine leaf extract, PF@AgNPs, and streptomycin was compared by measuring the diameter of inhibition zones (Figure 10). Compared to pristine leaf extract, PF@AgNPs exhibited 2.5- to 3-fold greater antibacterial activity against all the bacteria. There are three possible reasons for the antibacterial activity of PF@AgNPs, viz., the innate antibacterial
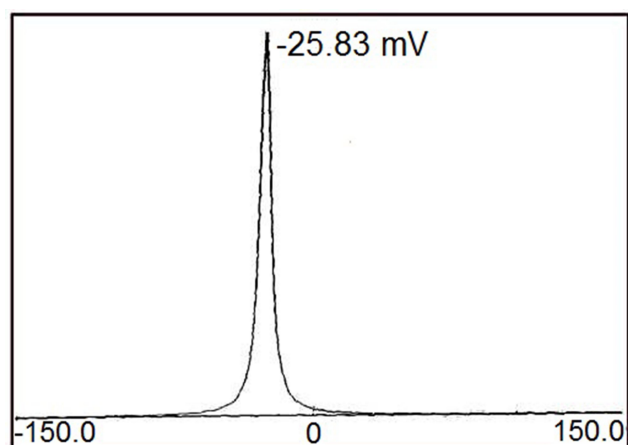
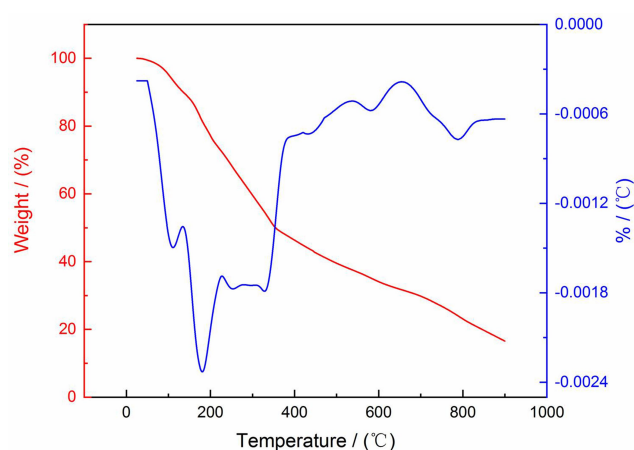**Figure 7** Zeta potential measurement of PF@AgNPs.

Figure 8 TG and DTG analysis PF@AgNPs.

nature of colloidal silver, the flavonoids, and polyphenols of the plant leaf extract may also contribute antibacterial activity and the ultrasmall size of nanoparticles, which

could easily penetrate the bacterial membrane and exhibit their action.[61,62] A possible antibacterial mechanism of PF@AgNPs is represented in the schematic diagram (Figure 11). AgNPs cause disruption of the peptidoglycan layer and lead to the formation of pores on the bacterial cell wall, through which AgNPs can enter the cell and exhibit their action. AgNPs interact with genomic DNA and cause DNA fragmentation, resulting in loss of the bacterial capacity for division/replication. AgNPs bind to bacterial enzymes/proteins and cause their inactivation/denaturation, which leads to the cessation of bacterial metabolism. AgNPs bind to the 70S ribosomal-mRNA-complex, which results in dissociation of ribosomal sub-units and fragmentation of mRNA, thereby preventing bacterial protein synthesis. Important ions or cytoplasmic contents can be released through the pores on the bacterial cell wall, which alters the proton motive force (PMF)/electric potential of the bacterial membrane. Collectively, these actions of AgNPs synergistically lead to bacterial cell death. In a case study on the antibacterial effect of nanosilver against *E. coli* as a model of gram-negative bacteria, Sondi and Salopek-Sondi (2004) reported that the antibacterial activity is a result of the AgNP-generated cell wall pits, which increase the membrane permeability and inactivate the respiratory chain.[63] Jung et al (2014) reported a common antibacterial mechanism against both gram-negative and gram-positive bacteria, in which AgNPs bind with carboxyl and phosphate groups of the bacterial cell membrane, thereby altering the electric membrane potential, which causes leakage of ions/molecules and leads to cell death.[64] Feng et al (2000) reported that AgNPs interact with DNA and enzymes/proteins
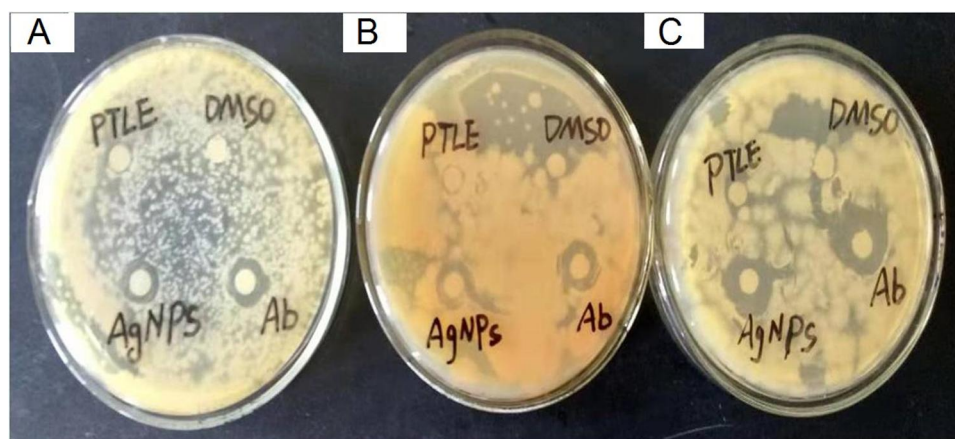

Figure 9 Antibacterial activity of PF@AgNPs against (**A**) *S. aureus*, (**B**) *B. subtilis*, and (**C**) *E. coli*; PTLE indicates pristine leaf extract; Ab indicates antibiotic; DMSO indicates dimethyl sulfoxide.
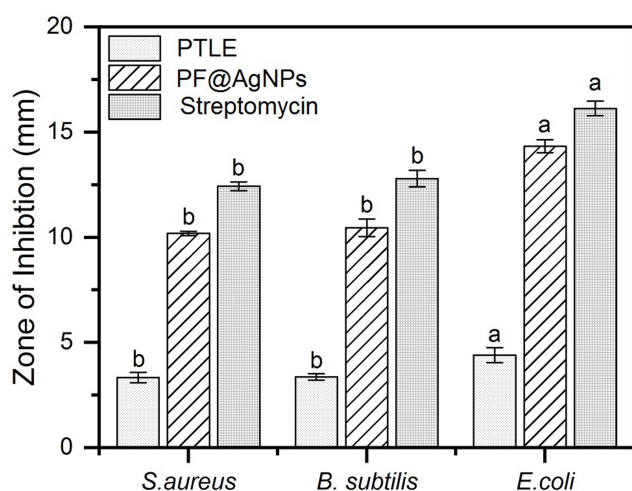
Figure 10 Comparison of antibacterial activity of pristine leaf extract (PTLE), PF@AgNPs and standard antibiotic streptomycin. Results were expressed as mean ± SD (n=3). Different lowercase letters above the bars indicate significant differences (P < 0.05) by SPSS test.
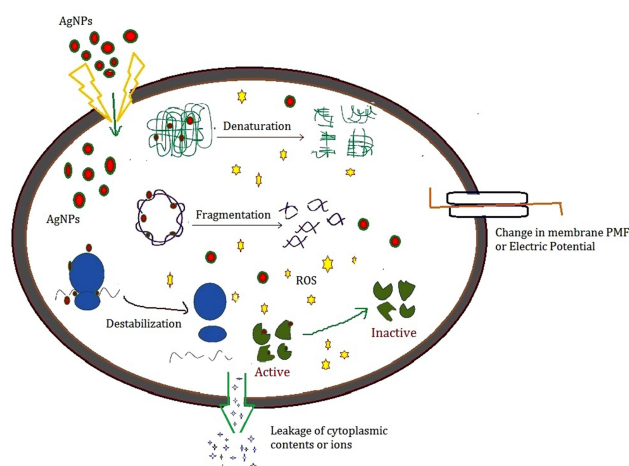

Figure 11 Scheme represents the possible mechanism of antibacterial activity of AgNPs.

involved in major metabolic pathways of bacteria leading to the cessation of bacterial metabolism and death of bacteria.[65] The results of the present study are supported strongly by previous reports. Mohammed et al (2018) reported that *Phoenix dactylifera, Ferula asafoetida*, and *Acacia nilotica* leaf-synthesized AgNPs exhibit antibacterial activity against both gram-positive (*S. aureus*) and gram-negative (*E. coli*) bacteria.[66] Elemike et al (2017) reported that pathogenic bacteria such as *S. aureus, E. coli, B. subtilis, Klebsiella pneumoniae*, and *Pseudomonas aeruginosa* were susceptible to phyto-synthesized AgNPs using *Costus afer*.[67] *Oedera genistifolia* leaf-synthesized AgNPs exhibit effective antibacterial activity against both gram-negative and gram-positive bacteria.[68]

In vitro Antioxidant Activity of the PF@AgNPs

The antioxidant activity of the PF@AgNPs was evaluated using ABTS and DPPH scavenging assays. The radical scavenging capacity of PF@AgNPs was concentration-dependent and increased with increasing concentration of PF@AgNPs from 20 to 100 μg/mL (Figure 12). PF@AgNPs exhibited a maximum scavenging capacity of 68.02% against DPPH radicals with an IC_{50} concentration of 54.52 μg/mL. PF@AgNPs also exhibited significant ABTS radical scavenging activity with a maximum inhibition of 62.93%. The IC_{50} concentration of PF@AgNPs against ABTS radicals was 66.86 μg/mL. The antioxidant activity of PF@AgNPs substantiates their applications in the biomedical and nutraceutical industries. AgNPs are widely used in the preparation of food packaging materials because of their
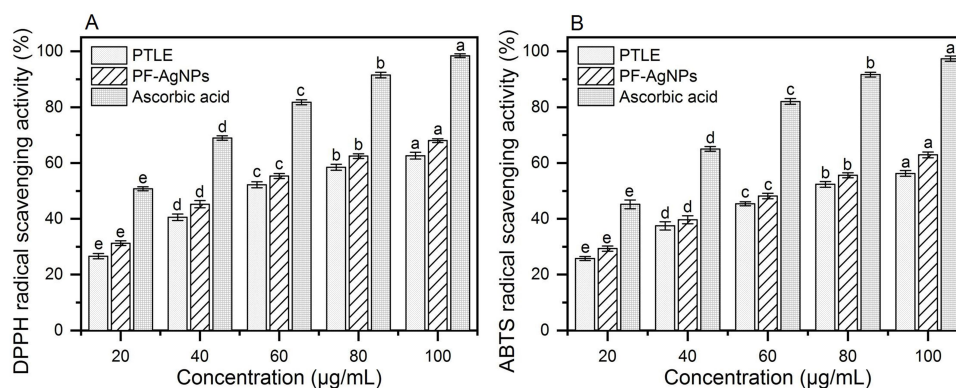

Figure 12 Antioxidant activities of PTLE, PF@AgNPs and ascorbic acid (**A**) DPPH radical scavenging activity, and (**B**) ABTS radical scavenging activity. All the data were represented as mean ± SD (n =3) in the form of bar graph. Data were analyzed by one-way analysis of variance (ANOVA, P < 0.05). Different lowercase letters above the bars indicate significant differences (P < 0.05).

antioxidant and antimicrobial activities. Various internal and external factors cause oxidative stress through the production of reactive oxygen species. Oxidative stress is associated with different diseases, including cancer, cardiovascular, neurological, and aging-related diseases, and antioxidants protect the body by reducing oxidative stress.[69] In recent years, scientists have focused on natural antioxidants because of the unknown side effects of synthetic drugs. Various phytochemicals such as polyphenols and, flavonoids, are known to play a major role in the synthesis and capping of AgNPs. Different polyphenols and flavonoids including caffeic acid, rosmarinic acid, gallic acid, ferulic acid, luteolin, apigenin, quercetin, and genistein are already reported in the aqueous extracts of *P. frutescens*. All of these molecules are natural antioxidants with strong radical scavenging activities.[31,70,71] Thus, the natural antioxidant capacity of phytosynthesized AgNPs has become an important property for their application in the biomedical, nutraceutical, and pharmaceutical fields.

Anticancer Activity of PF@AgNPs

The anticancer activity of the PF@AgNPs was evaluated using the cell lines COLO205 and LNCaP. PF@AgNPs showed anticancer activity in a concentration-dependent manner. An increase in the concentration of PF@AgNPs significantly reduced the cell viability of both COLO205 and LNCaP (Figure 13). PF@AgNPs exhibited maximum inhibition of 91.6 and 87.9% cell viability of LNCaP and COLO205 cells at the highest concentration (100 μg/mL) used in this study. The IC_{50} concentrations of PF@AgNPs against COLO205 and LNCaP were determined as 39.28
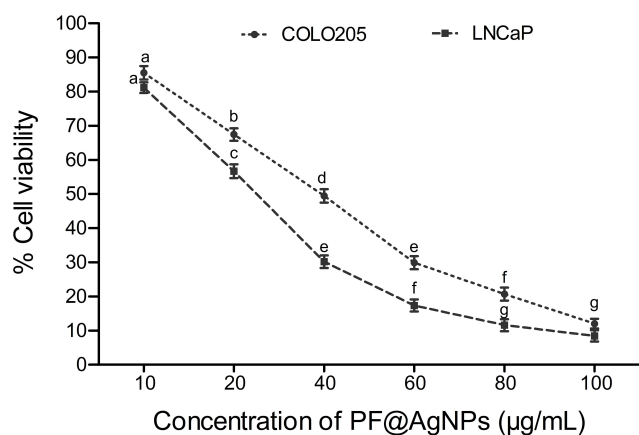

Figure 13 Dose-dependent cytotoxic effects of PF@AgNPs against human colon carcinoma (COLO205) and prostate carcinoma (LNCaP) All the data were represented as mean ± SD (n =3) in the form of bar graph. Bars with different superscripts indicate significant differences (P < 0.05).

and 24.33 μg/mL, respectively. Thus, LNCaP cells were more susceptible than COLO205 cells to the PF@AgNPs. Further morphological abnormalities in the most susceptible LNCaP cells were investigated under a phase-contrast microscope. Cells treated with $IC_{25,}$ $IC_{50,}$ and IC_{75} concentration of phytosynthesized AgNPs for 24 h showed noticeable morphological changes in a concentration-dependent manner (Figure 14). The morphological abnormalities include cell shrinkage, membrane destruction, chromatin condensation, protrusion of microspikes, fragmentation of nuclei, and formation of apoptotic bodies. However, the control cells showed healthy morphology with intact nuclei and no abnormalities. The results were supported by previous reports. Phytosynthesized AgNPs using *Mentha arvensis* and showed anticancer activity against colon cancer cell lines by exhibiting apoptotic effects, cell membrane fragmentation, and cell cycle suspension.[72] Phytosynthesized AgNPs using *Clinacanthus nutans* showed cytotoxic effects including membrane blebbing, nuclear fragmentation, and chromatin condensation of oral squamous cancer cells.[73]

Conclusions

In the present study, we report the bioreduction of silver ions into silver nanoparticles using *P. frutescens* aqueous leaf extract, which acts as both a reducing and capping agent for PF@AgNPs. The successful synthesis of PF@AgNPs was indicated by the color change and UV–Vis absorption peak. FTIR analysis demonstrated that polyphenols, flavonoids, and proteins play a major role in this bioreduction process. The physical properties of PF@AgNPs, such as size, shape, crystallinity, dispersity, surface charge, and stability were studied using a range of spectroscopic techniques, including TEM, XRD, DLS, and TGA. Different shapes of PF@AgNPs were detected, including spherical, triangle, rhombic, and rod shapes. The crystallite size was 25.71 nm with an FCC lattice. The high negative surface charge (−25.83 mV) indicated long-term stability with no aggregation. TEM micrograph and lower PI (0.389) value revealed the monodispersity of PF@AgNPs. PF@AgNPs were found to be thermostable with very low weight loss even at high temperatures. PF@AgNPs produced the maximum inhibition zone against *E. coli*, followed by *B. subtilis* and *S. aureus*. PF@AgNPs showed significant antioxidant activity by quenching DPPH and ABTS-free radicals. PF@AgNPs significantly reduced the cell viability of both COLO205 and LNCaP cancer cell lines. The apoptotic effects of
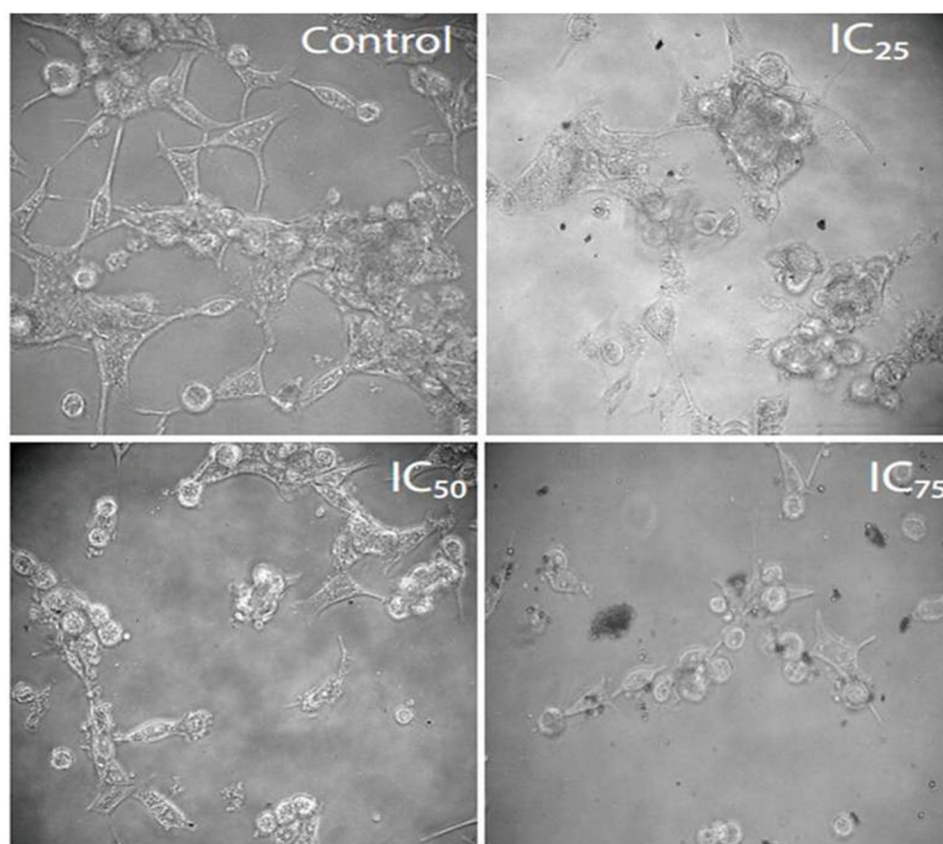
Figure 14 Anticancer activity of PF@AgNPs against LNCaP cell lines. The effects of PF@AgNPs on morphological changes of LNCaP cells were studied after 24 h exposure at different concentrations. PF@AgNPs affected the cell viability by inducing apoptotic symptoms, including warping of cells, rounding of cells, membrane blebbing, and cell shrinkage.

PF@AgNPs in the most susceptible LNCaP cells were observed and revealed the morphological changes, including rounded up cells, chromatin condensation, protrusion of microspikes, fragmentation of nucleus, and formation of apoptotic bodies. Thus, AgNPs were successfully synthesized using *P. frutescens* aqueous leaf extract, and we report their characterization, and antibacterial, antioxidant, and anticancer activities. The possible mechanisms of the bioreduction process and the antibacterial activity of green synthesized AgNPs are explained.

Highlights of the Manuscript

- *Perilla frutescens* leaf extract act as reducing and capping agent involved in the synthesis and stabilization of silver nanoparticles.
- *P. frutescens* leaf synthesized AgNPs (PF@AgNPs) are irregular shaped, face centered cubic crystallites, monodispersed, long term stable, and non-agglomerated.
- PF@AgNPs showed antibacterial activity against both gram-positive and gram-negative bacteria.

- PF@AgNPs exhibited significant free radical scavenging activity on ABTS and DPPH radicals.
- PF@AgNPs exhibited significant anticancer activity against human colon cancer and prostate adenocarcinoma.
- PF@AgNPs showed significant cytotoxic effects including nuclear fragmentation, membrane blebbing, and chromatin condensation of prostate cancer cells.

Ethical Statement

No animals were used/harmed for the present study. The cell lines including human colon cancer (COLO205) and prostate cancer (LNCaP) cells were commercially purchased from National Centre for Cellular Sciences, Pune, India.

Acknowledgments

Chemical Engineering Technology, North University of China) for her efforts in the statistical analysis of data, and drawing graphs.

Disclosure

All the authors report no conflicts of interest in this work.

References

1. Jo DH, Kim JH, Lee TG, Kim JH. Size, surface charge, and shape determine therapeutic effects of nanoparticles on brain and retinal diseases. *Nanomedicine*. 2015;11:603–1611. doi:10.1016/j.nano.2015. 04.015
2. Evanoff DD, Chumanov G. Synthesis and optical properties of silver nanoparticles and arrays. *Chem Phys Chem*. 2005;6:1221–1231. doi:10.1002/cphc.200500113
3. Salata O. Applications of nanoparticles in biology and medicine. *J Nanobiotechnology*. 2004;2(1):3. doi:10.1186/1477-3155-2-3
4. Natsuki J, Natsuki T, Hashimoto Y. A review of silver nanoparticles: synthesis methods, properties and applications. *Int J Mater Sci Appl*. 2015;4(5):325–332. doi:10.11648/j.ijmsa.20150.405.17
5. Zhang XF, Liu ZG, Shen W, Gurunathan S. Silver nanoparticles: synthesis, characterization, properties, applications, and therapeutic approaches. *Int J Mol Sci*. 2016;17(9):1534. doi:10.3390/ijms17091534
6. Syafiuddin A, Salim MR. A review of silver nanoparticles: research trends, global consumption, synthesis, properties, and future challenges. *J Chinese Chem Soc*. 2017;64(7):732–756. doi:10.1002/jccs.201700067
7. Pareek V, Gupta R, Panwar J. Do physico-chemical properties of silver nanoparticles decide their interaction with biological media and bactericidal action? A review. *Mater Sci Eng C Mater Biol Appl*. 2018;90:739–749. doi:10.1016/j.msec.2018.04.093
8. Kalantari K, Mostafavi E, Afifi AM, et al. Wound dressings functionalized with silver nanoparticles: promises and pitfalls. *Nanoscale*. 2020;12(4):2268–2291. doi:10.1039/c9nr08234d
9. Furno F, Morley KS, Wong B, et al. Silver nanoparticles and polymeric medical devices: a new approach to prevention of infection? *J Antimicrob Chemother*. 2004;54(6):1019–1024. doi:10.1093/jac/dkh478
10. Hamdan S, Pastar I, Drakulich S, et al. Nanotechnology-driven therapeutic interventions in wound healing: potential uses and applications. *ACS Cent Sci*. 2017;3(3):163–175. doi:10.1021/acs.centsci.6b00371
11. Chernousova S, Epple M. Silver as antibacterial agent: ion, nanoparticle, and metal. *Angew Chem Int Ed Engl*. 2013;52(6):1636–1653. doi:10.1002/anie.201205923
12. Fathi-Achachelouei M, Knopf-Marques H. Use of nanoparticles in tissue engineering and regenerative medicine. *Front Bioeng Biotechnol*. 2019;7:113. doi:10.3389/fbioe.2019.00113
13. Marassi V, Di Cristo L, Smith SGJ, et al. Silver nanoparticles as a medical device in healthcare settings: a five-step approach for candidate screening of coating agents. *R Soc Open Sci*. 2018;5 (1):171113. doi:10.1098/rsos.171113
14. Sawhney APS, Condon B, Singh KV, Pang SS, Li G, Hui D. Modern applications of nanotechnology in textiles. *Textile Res J*. 2008;78 (8):731–739. doi:10.1177/0040517508091066
15. Marin S, Vlasceanu GM, Tiplea RE, et al. Applications and toxicity of silver nanoparticles: a recent review. *Curr Top Med Chem*. 2015;15(16):1596–1604. doi:10.2174/1568026615666150414.4142 209
16. Lee J, Mahendra S, Alvarez PJ. Nanomaterials in the construction industry: a review of their applications and environmental health and safety considerations. *ACS Nano*. 2010;4(7):3580–3590. doi:10.1021/nn100866w

17. Tavakoli H, Rastegar H, Taherian M, Samadi M, Rostami H. The effect of nano-silver packaging in increasing the shelf life of nuts: an *in vitro* model. *Ital J Food Saf*. 2017;6(4):6874. doi:10.4081/ijfs.2017.6874
18. He X, Deng H, Hwang HM. The current application of nanotechnology in food and agriculture. *J Food Drug Anal*. 2019;27(1):1–21. doi:10.1016/j.jfda.2018.12.002
19. Abbasi E, Milani M, Fekri Aval S, et al. Silver nanoparticles: synthesis methods, bio-applications and properties. *Crit Rev Microbiol*. 2016;42(2):173–180. doi:10.3109/1040841X.2014.912200
20. Ray PC, Yu H, Fu PP. Toxicity and environmental risks of nanomaterials: challenges and future needs. *J Environ Sci Health C Environ Carcinog Ecotoxicol Rev*. 2009;27(1):1–35. doi:10.1080/10590500 802708267
21. Barkat MA, Harshita BS, et al. Current progress in synthesis, characterization and applications of silver nanoparticles: precepts and prospects. *Recent Pat Antiinfect Drug Discov*. 2018;13(1):53–69. doi:10.2174/1574891X12666171006102833
22. Mousavi SM, Hashemi SA, Ghasemi Y, et al. Green synthesis of silver nanoparticles toward bio and medical applications: review study. *Artif Cells Nanomed Biotechnol*. 2018;46(sup3):S855–S872. doi:10.1080/21691401.2018.1517769
23. Hamburger M, Hostettmann K. Bioactivity in plants: the link between phytochemistry and medicine. *Phytochemistry*. 1991;30:3864–3874. doi:10.1016/0031-9422(91)83425-K
24. Cragg GM, Newman DJ, Snader KM. Natural products in drug discovery and development. *J Nat Prod*. 1997;60:52–60. doi:10.1021/np9604893
25. Kamei R, Fujimura T, Matsuda M, et al. A flavanone derivative from the Asian medicinal herb (Perilla frutescens) potently suppresses IgE-mediated immediate hypersensitivity reactions. *Biochem Biophys Res Commun*. 2017;483(1):674–679. doi:10.1016/j.bbrc.2016.12.083
26. Takano H, Osakabe N, Sanbongi C, et al. Extract of *Perilla frutescens* enriched for rosmarinic acid, a polyphenolic phytochemical inhibits seasonal allergic rhinoconjuncti vitis in humans. *Exp Biol Med*. 2004;229:247–254. doi:10.1177/153537020422900305
27. Šmelcerović A, Tomović K, Šmelcerović Ž, et al. Xanthine oxidase inhibitors beyond allopurinol and febuxostat; an overview and selection of potential leads based on in silico calculated physico-chemical properties, predicted pharmacokinetics and toxicity. *Eur J Med Chem*. 2017;135:491–516. doi:10.1016/j.ejmech.2017.04.031
28. Ha TJ, Lee JH, Lee MH, et al. Isolation and identification of phenolic compounds from the seeds of *Perilla frutescens* (L.) and their inhibitory activities against α-glucosidase and aldose reductase. *Food Chem*. 2012;135(3):1397–1403. doi:10.1016/j.foodchem.2012.05.104
29. Verspohl EJ, Fujii H, Homma K, Buchwald-Werner S. Testing of *Perilla frutescens* extract and Vicenin 2 for their antispasmodic effect. *Phytomedicine*. 2013;20(5):427–431. doi:10.1016/j.phymed.2012.12.018
30. You CX, Yang K, Wu Y, et al. Chemical composition and insecticidal activities of the essential oil of *Perilla frutescens* (L.) Britt. aerial parts against two stored product insects. *Eur Food Res Technol*. 2014;239(3):481–490. doi:10.1007/s00217-014-2242-8
31. Yu H, Qiu JF, Ma LJ, Hu YJ, Li P, Wan JB. Phytochemical and phytopharmacological review of *Perilla frutescens* L. (Labiatae), a traditional edible-medicinal herb in China. *Food Chem Toxicol*. 2017;108(PtB):375–391. doi:10.1016/j.fct.2016.11.023
32. Oates PJ, Mylari BL. Aldose reductase inhibitors: therapeutic implications for diabetic complications. *Expert Opin Investig Drugs*. 1999;8(12):2095–2119. doi:10.1517/13543784.8.12.2095
33. Jeon IH, Kim HS, Kang HJ, et al. Anti-inflammatory and antipruritic effects of luteolin from Perilla (*P. frutescens* L.) leaves. *Molecules*. 2014;19(6):6941–6951. doi:10.3390/molecules19066941
34. Nakazawa T, Yasuda T, Ueda J, Ohsawa K. Antidepressant-like effects of apigenin and 2,4,5-trimethoxycinnamic acid from Perilla frutescens in the forced swimming test. *Biol Pharm Bull*. 2003;26 (4):474–480. doi:10.1248/bpb.26.474

35. Makino T, Furuta Y, Wakushima H, Fujii H, Saito K, Kano Y. Anti-allergic effect of *Perilla frutescens* and its active constituents. *Phytother Res*. 2003;17(3):240–243. doi:10.1002/ptr.1115

36. Li HZ, Ren Z, Reddy NV, Hou T, Zhang Z. *In silico* evaluation of antimicrobial, antihyaluronidase and bioavailability parameters of rosmarinic acid in *Perilla frutescens* leaf extracts. *SN Appl Sci*. 2020;2:1547. doi:10.1007/s42452-020-03323-8

37. Saifullah AS, Ahmad M, Swami BL, Ikram S. Green synthesis of silver nanoparticles using *Azadirachta indica* aqueous leaf extract. *J Radiation Res Appl Sci*. 2016;9:1–7. doi:10.1016/j.jrras.2015.06.006

38. Arokiyaraj S, Vincent S, Saravanan M, Lee Y, Young KO, Kim KH. Green synthesis of silver nanoparticles using *Rheum palmatum* root extract and their antibacterial activity against *Staphylococcus aureus* and *Pseudomonas aeruginosa*. *Artif Cells Nanomed Biotechnol*. 2017;45(2):372–379. doi:10.3109/21691401.2016.1160403

39. Singh P, Kim YJ, Singh H, et al. Biosynthesis, characterization, and antimicrobial applications of silver nanoparticles. *Int J Nanomedicine*. 2015;10:2567–2577. doi:10.2147/IJN.S72313

40. Ashour AA, Raafat D, El-Gowelli HM, El-Kamel AH. Green synthesis of silver nanoparticles using cranberry powder aqueous extract: characterization and antimicrobial properties. *Int J Nanomedicine*. 2015;10:7207–7221. doi:10.2147/IJN.S87268

41. Zia F, Ghafoor N, Iqbal M, Mehboob S. Green synthesis and characterization of silver nanoparticles using *Cydonia oblong* seed extract. *Appl Nanosci*. 2016;6:1023–1029. doi:10.1007/s13204-016-0517-z

42. Sun W, Qu D, Ma Y, Chen Y, Liu C, Zhou J. Enhanced stability and antibacterial efficacy of a traditional Chinese medicine-mediated silver nanoparticle delivery system. *Int J Nanomedicine*. 2014;9:5491–5502. doi:10.2147/IJN.S71670

43. Majeed Khan MA, Kumar S, Ahamed M, Alrokayan SA, Alsalhi MS. Structural and thermal studies of silver nanoparticles and electrical transport study of their thin films. *Nanoscale Res Lett*. 2011;6(1):434. doi:10.1186/1556-276X-6-434

44. Khan MJ, Shameli K, Sazili AQ, Selamat J, Kumari S. Rapid green synthesis and characterization of silver nanoparticles arbitrated by curcumin in an alkaline medium. *Molecules*. 2019;24(4):719. doi:10.3390/molecules24040719

45. Bhat RS, Almusallam J, Al Daihan S, Al-Dbass A. Biosynthesis of silver nanoparticles using *Azadirachta indica* leaves: characterization and impact on *Staphylococcus aureus* growth and glutathione-S-transferase activity. *IET Nanobiotechnology*. 2019;13(5):498–502. doi:10.1049/iet-nbt.2018.5133

46. Bauer AW, Kirby WM, Sherris JC, Turck M. Antibiotic susceptibility testing by a standardized single disk method. *Am J Clin Pathol*. 1966;45(4):493–496. doi:10.1093/ajcp/45.4_ts.493

47. LI HZ, Zhang Z, Jiao X. Optimization of ultrasound-assisted extraction of phenolic compounds, antioxidants and rosmarinic acid from perilla leaves using response surface methodology. *Food Sci Technol*. 2016;36:686–693. doi:10.1590/1678-457x.13516

48. Re R, Pellegrini N, Proteggente A, Pannala A, Yang M, Rice-Evans C. Antioxidant activity applying an improved ABTS radical cation decolorization assay. *Free Radic Biol Med*. 1999;26(9–10):1231–1237. doi:10.1016/s0891-5849(98)00315-3

49. Mosmann T. Rapid colorimetric assay for cellular growth and survival: application to proliferation and cytotoxicity assays. *J Immunol Methods*. 1983;65(1–2):55–63. doi:10.1016/0022-1759(83)90303-4

50. Kelly KL, Coronando E, Zhao LL, Schatz GC. The Optical properties of metal nanoparticles: the influence of size, shape and dielectric environment. *J Phys Chem B*. 2002;107:668–677. doi:10.1021/jp026731y

51. Das S, Das J, Samadder A, Bhattacharyya SS, Das D, Khuda-Bukhsh AR. Biosynthesized silver nanoparticles by ethanolic extracts of *Phytolacca decandra, Gelsemium sempervirens, Hydrastis canadensis* and *Thuja occidentalis* induce differential cytotoxicity through G2/M arrest in A375 cells. *Colloids Surf B Biointerfaces*. 2013;101:325–336. doi:10.1016/j.colsurfb.2012.07.008

52. Tran TT, Vu TT, Nguyen TH. Biosynthesis of silver nanoparticles using *Tithonia diversifolia* leaf extract and their antimicrobial activity. *Mater Lett*. 2013;105:220–223. doi:10.1016/j.matlet.2013.04.021

53. Mousavi B, Tafvizi F, Zaker Bostanabad S. Green synthesis of silver nanoparticles using *Artemisia turcomanica* leaf extract and the study of anti-cancer effect and apoptosis induction on gastric cancer cell line (AGS). *Artif Cells Nanomed Biotechnol*. 2018;46(sup1):499–510. doi:10.1080/21691401.2018.1430697

54. Simić A, Manojlović D, Segan D, Todorović M. Electrochemical behavior and antioxidant and prooxidant activity of natural phenolics. *Molecules*. 2007;12(10):2327–2340. doi:10.3390/121023.27

55. Gavade NL, Kadam AN, Suwarnkar MB, Ghodake VP, Garadkar KM. Biogenic synthesis of multi-applicative silver nanoparticles by using *Ziziphus Jujuba* leaf extract. *Spectrochim Acta A Mol Biomol Spectrosc*. 2015;136(Pt B):953–960. doi:10.1016/j.saa.2014.09.118

56. Ali M, Kim B, Belfield KD, Norman D, Brennan M, Ali GS. Green synthesis and characterization of silver nanoparticles using *Artemisia absinthium* aqueous extract–A comprehensive study. *Mater Sci Eng C Mater Biol Appl*. 2016;58:359–365. doi:10.1016/j.msec.2015.08.045

57. Behravan M, Hossein Panahi A, Naghizadeh A, Ziaee M, Mahdavi R, Mirzapour A. Facile green synthesis of silver nanoparticles using *Berberis vulgaris* leaf and root aqueous extract and its antibacterial activity. *Int J Biol Macromol*. 2019;124:148–154. doi:10.1016/j.ijbiomac.2018.11.101

58. Oliveira GZS, Lopes CAP, Sousa MH, Silva LP. Synthesis of silver nanoparticles using aqueous extracts of *Pterodon emarginatus* leaves collected in the summer and winter seasons. *Int Nano Lett*. 2019;9:109–117. doi:10.1007/s40089-019-0265-7

59. Khorrami S, Zarrabi A, Khaleghi M, Danaei M, Mozafari MR. Selective cytotoxicity of green synthesized silver nanoparticles against the MCF-7 tumor cell line and their enhanced antioxidant and antimicrobial properties. *Int J Nanomedicine*. 2018;13:8013–8024. doi:10.2147/IJN.S189295

60. Nasiriboroumand M, Montazer M, Barani H. Preparation and characterization of biocompatible silver nanoparticles using pomegranate peel extract. *J Photochem Photobiol B*. 2018;179:98–104. doi:10.1016/j.jphotobiol.2018.01.006

61. Alexander JW. History of the medical use of silver. *Surg Infect*. 2009;10:289–292. doi:10.1089/sur.2008.9941

62. Ranghar S. Nanoparticle-based drug delivery systems: promising approaches against infections. *Brazilian Arch Biol Technol*. 2012;57:209–222. doi:10.1590/S1516-89132013005000011

63. Sondi I, Salopek-Sondi B. Silver nanoparticles as antimicrobial agent: A case study on *E. coli* as a model for Gram-negative bacteria. *J Colloid Interface Sci*. 2004;275:177–182. doi:10.1016/j.jcis.2004.02.012.

64. Jung WK, Koo HC, Kim KW, Shin S, Kim SH, Park YH. Antibacterial activity and mechanism of action of the silver ion in *Staphylococcus aureus* and *Escherichia coli*. *Appl Environ Microbiol*. 2008;74(7):2171–2178. doi:10.1128/AEM.02001-07

65. Feng QL, Wu J, Chen GQ, Cui FZ, Kim TN, Kim JO. A mechanistic study of the antibacterial effect of silver ions on *Escherichia coli* and *Staphylococcus aureus*. *J Biomed Mater Res*. 2000;52(4):662–668. doi:10.1002/1097-4636(20001215)52:4<662::aid-jbm10>3.0.co;2-3

66. Elemike EE, Fayemi OE, Ekennia AC, Onwudiwe DC, Ebenso EE. Silver nanoparticles mediated by *Costus afer* leaf extract: synthesis, antibacterial, antioxidant and electrochemical properties. *Molecules*. 2017;22(5):701. doi:10.3390/molecules22050701

67. Mohammed AE, Al-Qahtani A, Al-Mutairi A, Al-Shamri B, Aabed KF. Antibacterial and cytotoxic potential of biosynthesized silver nanoparticles by some plant extracts. *Nanomaterials*. 2018;8(6):382. doi:10.3390/nano8060382

68. Okaiyeto K, Ojemaye MO, Hoppe H, Mabinya LV, Okoh AI. Phytofabrication of silver/silver chloride nanoparticles using aqueous leaf extract of *Oedera genistifolia*: characterization and antibacterial potential. *Molecules*. 2019;24(23):4382. doi:10.3390/molecules24234382

69. Young I, Woodside J. Antioxidants in health and disease. *J Clin Pathol*. 2001;54:176–186. doi:10.1136/jcp.54.3.176

70. Akhtar MS, Panwar J, Yeoung-Sang Y. Biogenic synthesis of metallic nanoparticles by plant extracts. *ACS Sus Chem Eng*. 2013;1:591–602. doi:10.1021/sc300118u

71. Pratt DE. Natural antioxidants from plant material," in phenolic compounds in food and their effects on health II. *ACS Symposium Ser*. 2009;507:54–71. doi:10.1021/bk-1992-0507.ch005

72. Javed B, Mashwani ZU. Synergistic effects of physicochemical parameters on bio-fabrication of mint silver nanoparticles: structural evaluation and action against HCT116 colon cancer cells. *Int J Nanomedicine*. 2020;15:3621–3637. doi:10.2147/IJN.S254402

73. Yakop F, Abd Ghafar SA, Yong YK, et al. Silver nanoparticles *Clinacanthus Nutans* leaves extract induced apoptosis towards oral squamous cell carcinoma cell lines. *Artif Cells Nanomed Biotechnol*. 2018;46(sup2):131–139. doi:10.1080/21691.401.2018.1452750